

Specific and Fuzzy Interactions Cooperate in Modulating Protein Half-Life

Rashmi Sharma^{1,†}, Máté Demény^{1,†}, Viktor Ambrus¹, Sándor Balázs Király², Tibor Kurtán², Pietro Gatti-Lafranconi³ and Monika Fuxreiter¹

1 - MTA-DE Laboratory of Protein Dynamics, Department of Biochemistry and Molecular Biology, University of Debrecen, Debrecen, Hungary

2 - Department of Organic Chemistry, University of Debrecen, Debrecen, Hungary

3 - Department of Biochemistry, University of Cambridge, UK

Correspondence to Monika Fuxreiter: fmoni@med.unideb.hu

<https://doi.org/10.1016/j.jmb.2019.02.006>

Edited by Richard W. Kriwacki

Abstract

Protein degradation is critical for maintaining cellular homeostasis. The 20S proteasome is selective for unfolded, extended polypeptide chains without ubiquitin tags. Sequestration of such segments by protein partners, however, may provide a regulatory mechanism. Here we used the AP-1 complex to study how c-Fos turnover is controlled by interactions with c-Jun. We show that heterodimerization with c-Jun increases c-Fos half-life. Mutations affecting specific contact sites (L165V, L172V) or charge separation (E175D, E189D, K190R) with c-Jun both modulate c-Fos turnover, proportionally to their impact on binding affinity. The fuzzy tail beyond the structured b-HLH/ZIP domain (~165 residues) also contributes to the stabilization of the AP-1 complex, removal of which decreases c-Fos half-life. Thus, protein turnover by 20S proteasome is fine-tuned by both specific and fuzzy interactions, consistently with the previously proposed “nanny” model.

© 2019 Elsevier Ltd. All rights reserved.

Introduction

Precise protein quality control is crucial for all cellular processes. The proteasome system is responsible for selective degradation of proteins to eliminate damaged, dysfunctional, or foreign sequences and tightly regulate protein turnover [1,2]. Alterations in half-life affects proliferation, apoptosis, DNA repair, immune, and stress response, and aberrant protein homeostasis is associated with developmental problems, cancer, and neurodegenerative pathologies [3–5]. The 26S proteasome [6] consists of the 20S catalytic core for proteolysis of unfolded segments [7–9], and the 19S regulatory particle(s) to recognize substrates with poly-ubiquitin tags [10,11]. The unstructured initiation sites exhibit biased amino acid compositions, which modulate the affinity for the proteasome [12]. Certain sequence signatures (e.g., low-complexity motifs), however, may increase stability of unfolded segments and selectively inhibit proteolysis [13,14].

Proteomic analysis of the 20S substrates revealed the enrichment of segments, which lack a well-defined tertiary structure in their native states [15]. Intrinsically disordered (ID) regions could be degraded by “default” via the 20S core particle, in accord with earlier proposals [16]. Indeed, proteins possessing long (≥ 30 residues) ID regions exhibit shorter half-life than those with shorter ID regions [17]. This presents a challenge for selective degradation: how to distinguish between non-functional, unfolded segments and exposed, dynamic, regulatory regions? Early observations indicated that turnover of inherently unstable proteins (e.g., ornithine decarboxylase) could be inhibited by complex formation with NAD(P)H quinone oxidoreductase 1 (NQO1) [18], which exerts a negative feedback for the 20S proteasome [19]. NQO1 is a ubiquitous enzyme that can also stabilize p53 and p73 α transcription factors to inhibit degradation [16].

Generalization of these observations leads to the proposal, that protein interactions might shield exposed, disordered regions and make them

inaccessible to the 20S catalytic machinery [20]. The survival of proteins with inherently unstable regions thus depends on the availability of their interacting partners (“nannies”) [20]. In accord, the experimentally determined 20S proteome has an increased interaction capacity [15], which potentially regulates the degradation by the 20S proteasome. Although individual examples where complexation extends protein half-life (e.g., $\text{IkB}\alpha$ -NF κ B [21], Ku70-Ku80 [22]) have been documented, the detailed molecular mechanisms remained to be elucidated.

We used the activator protein 1 (AP-1) model system to study the relationship between protein interactions and half-life. AP-1 regulates a number of cellular processes including differentiation, proliferation, and apoptosis via controlling gene expression in response to a plethora of signals, including cytokines, growth factors, stress, and viral infections [23]. AP-1 is a heterodimer that is composed of proteins belonging to the c-Fos and c-Jun families [24]. The c-Fos transcription factor has a short half-life [25], which could be elongated by its partner, c-Jun as well as by the 20S proteasome “gatekeeper” NQO1 [26,27]. Multiple pieces of evidence demonstrate that c-Fos is degraded by different mechanisms, also independently from ubiquitination [28–30]. Here we investigated how c-Fos turnover is modulated by specific mutations at contact sites with c-Jun and by the presence of the unstructured tail. Our results demonstrate that both specific and transient, nonspecific interactions influence half-life and propose a mechanism to regulate protein degradation via fine-tuning the interaction affinities with a binding partner.

Results

Mutant design

The structure of the AP-1 complex is a coiled-coil (PDB code: 1fos, [31]), which is held together by interdigitating hydrophobic contacts (“leucine zipper”). These are complemented by salt bridges at specific positions, which stabilize heterodimers as compared to homodimers. We designed five mutants using the full-length c-Fos: two affecting the hydrophobic network (L165V, L172V) and three perturbing the hydrophilic contacts (E175D, E189D, K190R) (Fig. 1a). In case of L \rightarrow V and E \rightarrow D replacements, the smaller sidechains might cause deviations from the ideal geometry while maintaining the polarity of the interaction. The K \rightarrow R mutation introduces a bulkier sidechain with additional π interactions. The C-terminal region of c-Fos comprises three PEST sequences [32], which do not overlap with the designed mutations.

The crystal structure comprises only those segments of c-Fos and c-Jun (139–200 aa c-Fos and 263–324 aa c-Jun), which adopt a well-defined helical structure upon binding [31]. The C-terminal region of c-Fos, however, dynamically fluctuates among various conformations both in the free form [33] and bound to c-Jun [34]. This mode of assembly, with extensive conformational exchange upon partner interactions, is referred to as a fuzzy complex [35,36]. We also designed a truncation mutant (c-Fos $_{\Delta 214}$) to probe the effect of the fuzzy C-terminal tail of c-Fos (215–380 aa).

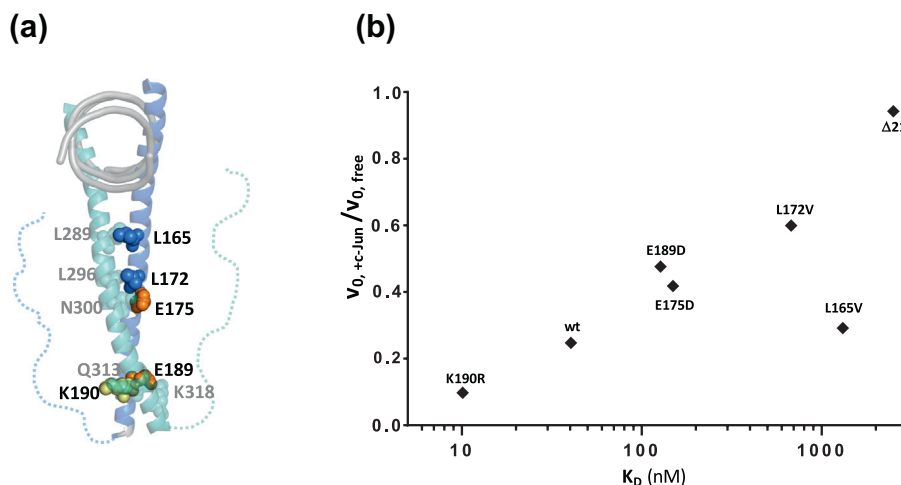


Fig. 1. (a) Designed mutations in the structure of the AP-1 complex (1.fos.pdb [31]). Mutations in c-Fos (marine, black labels) and the contacting residues in c-Jun (cyan, gray labels) are shown by spheres. Fuzzy C-terminal tails are displayed by dashed lines; the DNA is colored gray. (b) Change in c-Fos degradation rate via c-Jun interactions (v_{+c-Jun}/v_{free}) as a function of the binding affinity. The experimental K_D values are shown on a logarithmic scale.

Table 1. Propensity of unstructured secondary structure elements (%) as determined by ECD spectroscopy

	Unstructured (%)	
	Free	+ c-Jun
c-Fos	48.7	44.2
c-Jun	44.4	–
c-Fos _{L172V}	44.5	42.5
c-Fos _{E175D}	42.1	46.5
c-Fos _{Δ214}	46.2	47.1

ECD spectra were recorded on a J-810 spectropolarimeter in 20 mM sodium phosphate (pH 7.4) buffer solution with a 0.2-mm quartz cell at room temperature. Raw spectra were corrected with the blank, then were converted to mean residue ellipticities and were smoothed. Deconvolution was performed by the BeStSel program [63,64].

c-Fos forms a fuzzy complex with c-Jun

We applied electronic circular dichroism (ECD) spectroscopy to assess the impact of the mutations on c-Fos structure in the free form and in complex with full-length c-Jun (Table S1). In accord with previous experimental results, almost half of the residues in c-Fos (185 out of 380 aa) do not possess regular secondary structures and are disordered [33]. Interaction with c-Jun slightly increases the helical population of c-Fos as compared to the free state, but does not induce extensive ordering (Table 1). These data indicate that c-Fos forms a fuzzy complex with c-Jun, where 45.8 % of the residues remain to be disordered, consistently with previous FRET and FCCS results [34]. On the other hand, no substantial unfolding of the structured part takes place, as the number of residues with regular secondary conformations (>200 aa in full-length c-Fos, 113 aa in c-Fos_{Δ214}) exceeds the size of the bHLH/LZ (62 aa). The L172V and E175D substitutions cause only minor increase in the secondary structures of c-Fos (Table 1). Structural disorder of the c-Fos_{L172V} and c-Fos_{L175D} mutants is retained upon assembly with c-Jun, with small impact on the

secondary structure properties as compared to the wild-type protein. Secondary structure predictions by the GOR IV algorithm [37] suggest a considerable reduction in helicity in c-Fos_{L165V} as compared to the wild-type protein or c-Fos_{L172V} (Table S2).

Deletion of the disordered C-terminal region (215–380 aa) has a negligible impact on c-Fos structure (Table 1). This is due to the removal of only 166 out of 323 disordered residues. The remaining unstructured fraction also includes a 15-residue disordered segment flanking the leucine zipper (200–214 aa), which reduces termination effects. Interactions with full-length c-Jun have a moderate influence on the secondary structure properties of c-Fos_{Δ214}. Taken together, c-Fos and all the studied variants form a fuzzy complex with c-Jun and do not completely fold upon binding.

Both specific and fuzzy interactions modulate binding affinity

To assess the effect of binding affinity on the degradation rate of c-Fos, specific contacts between c-Fos/c-Jun complex were perturbed (Fig. 1a). In contrast to most previous studies (Table S3 and references therein), we used the full-length c-Fos (380 aa) and c-Jun (331 aa) to investigate the interplay between the specific interactions by the structured elements and the transient interactions by the fuzzy tail. All substitutions decrease binding affinity by less than 2 orders of magnitude, except the K190R mutation (Table 2). Perturbing the hydrophobic interface (L165V, L172V) has the most considerable effect on the stability of the complex due to looser zipper contacts. Reducing the size of the negatively charged residues (E175D, E189D) has a moderate impact on K_D due to weaker electrostatic interactions. The K190R mutation slightly stabilizes the heterodimer via additional π - π interactions with Q313. Mutations in full-length c-Fos mostly affect the association kinetics, in line with previous data [38,39].

Table 2. Experimental binding affinities and computed interaction energies of c-Fos mutants with c-Jun

	k_a ($\times 10^3$ M ⁻¹ s ⁻¹)	k_d ($\times 10^4$ s ⁻¹)	K_D (nM)	Affinity ratio to wild type	$\Delta\Delta G_{int}^{wt-mut}$ (kcal/mol)
c-Fos	80.30 ± 18.50	32.40 ± 1.95	40.4 ± 22.6	–	–
c-Fos _{L165V}	1.82 ± 0.038	23.80 ± 0.90	1310 ± 73.8	0.03	0.77
c-Fos _{L172V}	8.16 ± 0.20	55.10 ± 2.28	676 ± 79.7	0.06	1.51
c-Fos _{E175D}	7.76 ± 0.12	11.60 ± 0.74	149 ± 85.3	0.27	0.01
c-Fos _{E189D}	5.53 ± 0.064	7.02 ± 0.47	127 ± 125	0.32	-0.01
c-Fos _{K190R}	76.40 ± 0.88	7.75 ± 0.48	10.1 ± 5.79	4.0	-0.17
c-Fos _{Δ214}	3.11 ± 0.42	77.80 ± 1.44	2500 ± 511	0.02	–

Association and dissociation curves were determined at 37 °C by BLITZ analysis [62] using a 1:1 binding model. c-Fos mutants were added to Jun-labeled biosensors in different concentrations. Jun was marked by 60A8 Jun antibody (Cell Signaling Technologies). The equilibrium dissociation constant was determined as $K_D = k_d/k_a$, where k_d is the dissociation and k_a is the association rate. $\Delta\Delta G_{int}^{wt-mut}$ was computed by the FoldX program [48]. Amino acid replacements were carried out on the 1fos.pdb structure [31], and mutated residues were subjected to short relaxation. As the fuzzy C-terminal tail of c-Fos was not included, the changes in interaction energy between the structured segments were computed.

Binding of full-length proteins without complete folding might exhibit complex kinetics [40,41] (and references therein) as compared to protein fragments, which become structured upon binding [42]. Therefore, inclusion of the fuzzy tails in full-length c-Fos (380 aa) and c-Jun (331 aa) improves binding affinity (40 nM, Table 2) as compared to the interactions between leucine zippers (63 aa, $K_D = 54$ nM, [43]). Indeed, removal of the disordered tail in c-Fos $_{\Delta 214}$ considerably destabilizes the dimer (Table 2). A similar trend has been observed in c-Max and c-Myc assembly, where the fuzzy tail masks the electrostatic repulsion between the coiled-coil regions [44,45].

Within the framework of the fly-casting model, disordered regions increase local concentration nearby the target via nonspecific (e.g., electrostatic) interactions [46,47]. Along these lines, fuzzy regions in protein complexes can serve as nonspecific anchors, which remain attached and decrease dissociation rates even in the absence of specific contacts [36]. Indeed, the removal of the fuzzy C-terminal region in c-Fos $_{\Delta 214}$ considerably increases the dissociation rate from c-Jun as compared to the wild-type protein (Table 2). Replacements of charged residues in full-length c-Fos also slow down the dissociation rates by 3- to 4-folds (Table 2), consistently with the fly-casting model. The more complex kinetics is also illustrated in case of the c-Fos $_{L165V}$ and c-Fos $_{L172V}$ mutants, where data could be fitted better using a two-state model (Table S4).

We also determined the changes in interaction energies ($\Delta\Delta G_{int}^{wt \rightarrow mut}$) using the FoldX program [48] based on the coiled-coil structure (1fos.pdb [31]). Although the computed $\Delta\Delta G_{int}^{wt \rightarrow mut}$ results qualitatively reproduce the experimental trends (i.e., the K190R mutation is stabilizing, and the L \rightarrow V mutations at the helix-helix interface are destabilizing), they are considerably smaller than those deduced from the experimental binding affinities of the full models. These results corroborate the interactions between fuzzy tail and the helical interface.

Changes in c-Fos degradation rates correlate to interaction strength

c-Fos is degraded via both ubiquitination and ubiquitin-independent mechanisms [25]. The disordered regions can contribute to both pathways [49], out of which the “default” degradation mechanism mediated by the 20S proteasome was addressed [16,26]. Using a purified proteasome assay [50,51], we followed c-Fos degradation in the absence and presence of c-Jun. The E \rightarrow D replacements stabilize the free c-Fos, whereas the K190R and $\Delta 214$ shorten c-Fos half-life. The initial degradation rates of free c-Fos, however, are not affected considerably by the site-specific mutations or C-terminal truncation (Table 3), consistently with moderate change in c-Fos structure (Tables 1 and S1). These results indicate that the mutations do not alter interactions with the 20S proteasome, and changes in c-Fos degradation are due to the partnership with c-Jun.

Interactions with c-Jun impair c-Fos degradation by the 20S proteasome, in accord with previous results [26]. All the mutations have a larger impact on c-Fos half-life in the presence than in the absence of c-Jun, indicating that interactions with the binding partner influence c-Fos degradation (Table 3). c-Fos turnover is prolonged in all cases, independently whether the mutation stabilize or destabilize the complex ($v_{+c-Jun}/v_{free} < 1$, Table 3). The impact on the initial degradation rates, however, parallels the interaction strength of the mutant (Table 3, Fig. 1b). Destabilizing the complex reduces the protecting role of the binding partner as compared to the wild-type. In accord, the destabilizing L172V mutation, which affects hydrophobic contacts, exhibits smaller decrease in the initial degradation rates than those affecting hydrophilic interactions (E175D, E189D). In contrast, the stabilizing K190R mutation slows down the initial degradation as compared to the wild-type c-Fos (Fig. 1b). The c-Fos $_{L165V}$, however, exhibits substantial deviation from these trends, owing to its considerably decreased helicity (Table S2) and decreased dissociation rates (Table 2).

Table 3. Half-lives and initial degradation rates of c-Fos in the absence and in the presence of c-Jun

	Half-life (min)		Initial degradation rate (O.D./min)		
	Free	+ c-Jun	Free ($\times 10^{-2}$)	+ c-Jun ($\times 10^{-2}$)	v_{+c-Jun}/v_{free}
c-Fos	11.64 \pm 0.44	19.18 \pm 9.00	3.00 \pm 0.14	0.74 \pm 0.60	0.247
c-Fos $_{L165V}$	10.84 \pm 0.13	14.16 \pm 3.74	3.46 \pm 0.04	1.01 \pm 0.22	0.292
c-Fos $_{L172V}$	10.93 \pm 3.53	15.69 \pm 2.76	3.31 \pm 0.77	1.98 \pm 0.46	0.598
c-Fos $_{E175D}$	23.95 \pm 2.35	23.67 \pm 7.90	3.08 \pm 0.18	1.29 \pm 0.30	0.419
c-Fos $_{E189D}$	17.36 \pm 1.15	20.73 \pm 2.32	3.07 \pm 0.09	1.46 \pm 0.66	0.476
c-Fos $_{K190R}$	9.28 \pm 2.86	151.95 \pm 33.87	2.46 \pm 0.72	0.24 \pm 0.08	0.097
c-Fos $_{\Delta 214}$	9.07 \pm 1.25	13.85 \pm 4.09	2.86 \pm 0.48	2.69 \pm 0.48	0.941

Degradation assays have been performed using purified human 20S proteasomes [50] by measuring c-Fos concentration at 0, 15, 40, and 80 min. Initial degradation rates were obtained by nonlinear data fitting of the decay curves using the R program. All reactions were run in triplicates. v_{+c-Jun}/v_{free} is the ratio of the initial degradation rates of c-Fos in the complex and the free form.

The presence of the c-Fos fuzzy tail also decreases the degradation rate almost by 4-fold (Table 3), consistently with its significant contribution to the stability of the AP-1 complex (Table 2). Thus, removal of the fuzzy C-terminal segment decreases c-Fos protection via weakening the complexation with c-Jun (Table 3). Taken together, although interaction affinity is likely to be the major determinant in stabilizing c-Fos, the relationship appears to be rather complex.

Discussion

The nanny hypothesis provides a plausible model for how regulatory regions, which do not adopt a folded structure, can survive degradation by the 20S proteasome machinery [20]. This model is particularly relevant for proteins with ID regions [52], which constitute about one third of the human proteome [53]. Although structural data indicate the lack of a compact structure also *in vivo* [54], persistence of this feature challenges the quality control mechanisms of the cell. A possible solution is to link the expression of an ID protein to an interacting partner, which can mask and thus protect the fluctuating, unfolded segment from degradation [20]. This may drive protein assembly *in vivo* [21,22], molecular details of which have remained to be enigmatic.

Here we aimed to explore how specificity and affinity of protein interactions influence degradation by the 20S proteasome. Using the AP-1 as a model system, we demonstrated that both hydrophobic and hydrophilic contacts at the helix–helix interface affect c-Fos degradation. We also showed that protection by the partner qualitatively correlates to the binding affinity, and destabilizing the assembly reduces the impact of the mutation on degradation rates. There are additional factors, however, that can also influence stabilization, for example, decreased dissociation rates, or steric effects (in larger systems, not studied here) indicating a rather complex protection mechanism. Taken together, these results suggest that protein turnover can be modulated via fine-tuning the association with a binding partner.

ECD measurements evidence that the C-terminal tail of c-Fos retains its disordered state in complex with c-Jun. This supports that protection of disordered regions can be achieved without inducing a stable structure, and many binding configurations could be visited in the bound state without decreasing the conformational entropy [36]. Thus, 20S proteasome degradation can be impaired via a fuzzy assembly between the nanny and its client(s) and may not require specific chaperones [55]. Consequently, fine-tuning the dynamics of fuzzy regions, for example, via post-translational modifications could significantly affect half-life [56,57].

The protective role of fuzzy interactions from the 20S proteasome could also provide a plausible explanation for how low-complexity sequence motifs might serve as selective inhibitors of proteolysis [13,14]. Tandem repeats of short, linear sequences are frequently associated with proteins, which form higher-order protein structures or undergo liquid–liquid phase transition [58]. Interactions between these motifs are often not specific or well defined, and multivalency [59] or fuzziness [60] is a ubiquitous feature of these associations. We may assume that such weak, heterogeneous contacts could also serve to protect disordered stretches with multivalent, low-complexity motifs [61] from the ubiquitin-independent degradation pathway.

Conclusion

Our work highlights a novel aspect of protein fuzziness in regulating of protein half-life. First, we demonstrate that protection of disordered regions from degradation could be achieved without inducing a stable structure. Binding to a partner generates a fuzzy complex, where significant conformational entropy is retained. Second, we show that both specific contacts and fuzzy interactions can impair protein degradation, proportionally to their contribution to binding affinity, suggesting that protein turnover can be regulated via fine-tuning protein assembly. Third, low-complexity motifs may selectively inhibit proteolysis by generating higher-order structures via fuzzy interactions, suggesting the role of membraneless cellular compartments in protecting disordered regions from degradation. Investigating this aspect of the model is ongoing in our laboratory.

Materials and Methods

Protein expression and purification

The coding sequences of human c-Fos (Uniprot: P01100), c-Fos $_{\Delta 214}$, and c-Jun (donated by Joerg Langowski, DKFZ in Heidelberg, Germany [34]) were cloned into the pET-Duet-1 vector. Site-directed mutagenesis was carried out by the QuikChange II Site-Directed Mutagenesis Kit (Agilent Technologies). Proteins were expressed in *Escherichia coli* bacterial cultures (Rosetta2(DE3) pLysS, Novagen) using IPTG induction for 3 h. Protein purification was performed by immobilized metal affinity chromatography using a Ni-Sepharose™ 6 Fast Flow resin (GE Healthcare) with a lysis buffer containing 250 mM imidazole. Proteins were dialyzed against 100 volumes of 4, 2, and 1 M urea consecutively, then the buffer was changed to

25 mM Tris–HCl (pH 7.4) and 100 mM NaCl. The eluted proteins were concentrated with an Amicon-Ultra 50 10000 MWCO ultrafiltration device. Protein concentrations were determined by BCA protein assay.

Determination of binding kinetics

The binding kinetics of c-Fos variants to c-Jun were measured with a BLItz (PALL-ForteBio) bio-layer interferometer [62]. c-Jun of 1.5 μ g was pre-complexed with 60A8 anti-Jun antibody (Cell Signaling Technologies) at 37 °C until saturation has been reached. The antibody does not compete with c-Jun for binding to c-Fos (c-Jun does not significantly reduce the signal intensity of 6A9 Ab in the ELISA assay, see below) and is not specific to the C-terminus (it can also detect the c-Fos $_{\Delta 214}$ variant). The complex was loaded onto Protein-A Dip and Read biosensors to a spectral shift of 3.5 nm. c-Fos variants were diluted into PBS containing 0.1% Tween-20 to various concentrations, and their association to c-Jun was measured before the biosensor was dipped into the same buffer to record the dissociation of the proteins. The binding curves were fitted to a 1:1 binding model using the BLItz Pro™ software.

In vitro 20S proteasome assay

c-Fos variants and human 20S proteasome (Boston Biochem, cat. no. E-360) were diluted in solution of 25 mM Tris–HCl (pH 7.5), 100 mM NaCl, and 0.5 mM DTT to concentrations of 400 nM (c-Fos) and 8 nM (20S proteasome). The degradation assay was performed by mixing 12.5 μ l of each solution. Degradation of the c-Fos was followed at 37 °C, and 2 μ l samples were collected at 0, 15, 40, and 80 min, which were transferred into a solution containing 98 μ l of PBS, 0.1% Tween-20, 1% BSA, 1 μ M PS341, and protease inhibitors (EDTA free protease inhibitor cocktail; Roche). The amount of c-Fos at each time point was determined using an ELISA assay. The c-Fos solution was loaded onto 96-well Pierce Nickel-coated plates (Thermo Scientific, cat. no. 15442) at 25 °C. After 1 h, the wells were washed with PBS–0.1% Tween-20 three times and 9F6 anti-cFos antibody (Cell Signaling Technologies, 0.002 dilution) was added. This was followed by a reaction with HRP-conjugated anti-rabbit IgG (1:1000) and tetramethyl-benzidine (Sigma, T4444). The reaction was terminated by 1 M HCl, and intensity was measured at $\lambda = 450$ nm using Synergy H1 microplate reader (BioTeK Instruments). Protein amounts were computed based on a calibration curve obtained with BSA-determined concentrations. Nonlinear fitting of the decay curves was performed by the R program using a 1:1 binding model. All reactions were run in triplicates.

Acknowledgment

We are indebted to Jörg Langowski (DKFZ, Heidelberg) for providing the Fos-EGFP and Jun-mRFP1 constructs in 2013, which have been used in our preliminary studies. Owing to his tragic accident in 2017, we dedicate the article to his memory. We also thank Krisztina Tar, Zsolt Bacsó, and György Vámosi for fruitful discussions and Barbara Sárkány for careful reading of the manuscript. The two-state model binding kinetics were evaluated by Bálint Bécsi. Financial support is provided by GINOP-2.3.2-15-2016-00044, HAS 11015, and the DE Excellence Program (M.F.). T. K. and S. B. K. thank the National Research, Development and Innovation Office (NKFI K120181) for financial support.

Appendix A. Supplementary data

Supplementary data to this article can be found online at <https://doi.org/10.1016/j.jmb.2019.02.006>.

Received 14 December 2018;

Received in revised form 24 January 2019;

Accepted 3 February 2019

Available online 18 February 2019

Keywords:

protein degradation;
20S proteasome;
AP-1 complex;
fuzzy complex;
nanny model

†RS and M.D. contributed equally to the work.

Abbreviations used:

ID, intrinsically disordered; NQO1, NAD(P)H quinone oxidoreductase 1; AP-1, activator protein 1; ECD, electronic circular dichroism.

References

- [1] A. Hershko, A. Ciechanover, The ubiquitin system, *Annu. Rev. Biochem.* 67 (1998) 425–479.
- [2] D. Voges, P. Zwickl, W. Baumeister, The 26S proteasome: a molecular machine designed for controlled proteolysis, *Annu. Rev. Biochem.* 68 (1999) 1015–1068.
- [3] M. Pagano, S.W. Tam, A.M. Theodoras, P. Beer-Romero, G. Del Sal, V. Chau, et al., Role of the ubiquitin–proteasome pathway in regulating abundance of the cyclin-dependent kinase inhibitor p27, *Science* 269 (1995) 682–685.
- [4] D. Hoeller, I. Dikic, Targeting the ubiquitin system in cancer therapy, *Nature* 458 (2009) 438–444.

- [5] A. Ciechanover, Intracellular protein degradation: from a vague idea thru the lysosome and the ubiquitin–proteasome system and onto human diseases and drug targeting, *Biochim. Biophys. Acta* 2011 (1824) 3–13.
- [6] X. Huang, B. Luan, J. Wu, Y. Shi, An atomic structure of the human 26S proteasome, *Nat. Struct. Mol. Biol.* 23 (2016) 778–785.
- [7] P.C. da Fonseca, E.P. Morris, Cryo-EM reveals the conformation of a substrate analogue in the human 20S proteasome core, *Nat. Commun.* 6 (2015) 7573.
- [8] P. Chen, M. Hochstrasser, Autocatalytic subunit processing couples active site formation in the 20S proteasome to completion of assembly, *Cell.* 86 (1996) 961–972.
- [9] S. Prakash, L. Tian, K.S. Ratliff, R.E. Lehotzky, A. Matouschek, An unstructured initiation site is required for efficient proteasome-mediated degradation, *Nat. Struct. Mol. Biol.* 11 (2004) 830–837.
- [10] T. Ravid, M. Hochstrasser, Diversity of degradation signals in the ubiquitin–proteasome system, *Nat. Rev. Mol. Cell Biol.* 9 (2008) 679–690.
- [11] S. Prakash, T. Inobe, A.J. Hatch, A. Matouschek, Substrate selection by the proteasome during degradation of protein complexes, *Nat. Chem. Biol.* 5 (2009) 29–36.
- [12] S. Fishbain, T. Inobe, E. Israeli, S. Chavali, H. Yu, G. Kago, et al., Sequence composition of disordered regions fine-tunes protein half-life, *Nat. Struct. Mol. Biol.* 22 (2015) 214–221.
- [13] A. Sharipo, M. Imreh, A. Leonchiks, S. Imreh, M.G. Masucci, A minimal glycine–alanine repeat prevents the interaction of ubiquitinated I kappaB alpha with the proteasome: a new mechanism for selective inhibition of proteolysis, *Nat. Med.* 4 (1998) 939–944.
- [14] H. Yu, A.K. Singh Gautam, S.R. Wilmington, D. Wylie, K. Martinez-Fonts, G. Kago, et al., Conserved sequence preferences contribute to substrate recognition by the proteasome, *J. Biol. Chem.* 291 (2016) 14526–14539.
- [15] N. Myers, T. Olender, A. Savidor, Y. Levin, N. Reuven, Y. Shaul, The disordered landscape of the 20S proteasome substrates reveals tight association with phase separated granules, *Proteomics* 18 (2018), e1800076.
- [16] G. Asher, N. Reuven, Y. Shaul, 20S proteasomes and protein degradation “by default”, *Bioessays* 28 (2006) 844–849.
- [17] R. van der Lee, B. Lang, K. Kruse, J. Gsponer, N. Sanchez de Groot, M.A. Huynen, et al., Intrinsically disordered segments affect protein half-life in the cell and during evolution, *Cell Rep* 8 (2014) 1832–1844.
- [18] G. Asher, Z. Bercovich, P. Tsvetkov, Y. Shaul, C. Kahana, 20S proteasomal degradation of ornithine decarboxylase is regulated by NQO1, *Mol. Cell* 17 (2005) 645–655.
- [19] O. Moscovitz, P. Tsvetkov, N. Hazan, I. Michaelevski, H. Keisar, G. Ben-Nissan, et al., A mutually inhibitory feedback loop between the 20S proteasome and its regulator, NQO1, *Mol. Cell* 47 (2012) 76–86.
- [20] P. Tsvetkov, N. Reuven, Y. Shaul, The nanny model for IDPs, *Nat. Chem. Biol.* 5 (2009) 778–781.
- [21] D. Krappman, F.G. Wulczyn, C. Scheidereit, Different mechanisms control signal induced degradation and basal turnover of the NF-kappaB inhibitor and inhibitor ikappaB alpha in vivo, *EMBO J.* 15 (1996) 6716–6726.
- [22] Y. Gu, K.J. Seidl, G.A. Rathbun, C. Zhu, J.P. Manis, N. van der Stoep, et al., Growth retardation and leaky SCID phenotype of Ku70-deficient mice, *Immunity* 7 (1997) 653–665.
- [23] R. Eferl, E.F. Wagner, AP-1: a double-edged sword in tumorigenesis, *Nat. Rev. Cancer* 3 (2003) 859–868.
- [24] Y. Chinenov, T.K. Kerppola, Close encounters of many kinds: Fos–Jun interactions that mediate transcription regulatory specificity, *Oncogene* 20 (2001) 2438–2452.
- [25] G. Bossis, P. Ferrara, C. Acquaviva, I. Jariel-Encontre, M. Piechaczyk, c-Fos proto-oncoprotein is degraded by the proteasome independently of its own ubiquitinylation in vivo, *Mol Cell Biol* 23 (2003) 7425–7436.
- [26] J. Adler, N. Reuven, C. Kahana, Y. Shaul, c-Fos proteasomal degradation is activated by a default mechanism, and its regulation by NAD(P)H:quinone oxidoreductase 1 determines c-Fos serum response kinetics, *Mol. Cell. Biol.* 30 (2010) 3767–3778.
- [27] P. Tsvetkov, N. Myers, O. Moscovitz, M. Sharon, J. Prilusky, Y. Shaul, Thermo-resistant intrinsically disordered proteins are efficient 20S proteasome substrates, *Mol. BioSyst.* 8 (2012) 368–373.
- [28] C. Acquaviva, C. Salvat, F. Brockly, G. Bossis, P. Ferrara, M. Piechaczyk, et al., Cellular and viral Fos proteins are degraded by different proteolytic systems, *Oncogene* 20 (2001) 942–950.
- [29] I. Jariel-Encontre, M. Pariat, F. Martin, S. Carillo, C. Salvat, M. Piechaczyk, Ubiquitinylation is not an absolute requirement for degradation of c-Jun protein by the 26 S proteasome, *J. Biol. Chem.* 270 (1995) 11623–11627.
- [30] I. Jariel-Encontre, C. Salvat, A.M. Steff, M. Pariat, C. Acquaviva, O. Furstoss, et al., Complex mechanisms for c-fos and c-jun degradation, *Mol. Biol. Rep.* 24 (1997) 51–56.
- [31] J.N. Glover, S.C. Harrison, Crystal structure of the heterodimeric bZIP transcription factor c-Fos-c-Jun bound to DNA, *Nature* 373 (1995) 257–261.
- [32] M. Rechsteiner, S.W. Rogers, PEST sequences and regulation by proteolysis, *Trends Biochem. Sci.* 21 (1996) 267–271.
- [33] K.M. Campbell, A.R. Terrell, P.J. Laybourn, K.J. Lumb, Intrinsic structural disorder of the C-terminal activation domain from the bZIP transcription factor Fos, *Biochemistry* 39 (2000) 2708–2713.
- [34] G. Vamosi, N. Baudendistel, C.W. von der Lieth, N. Szaloki, G. Mocsar, G. Muller, et al., Conformation of the c-Fos/c-Jun complex in vivo: a combined FRET, FCCS, and MD-modeling study, *Biophys. J.* 94 (2008) 2859–2868.
- [35] M. Fuxreiter, Fuzziness in protein interactions—a historical perspective, *J. Mol. Biol.* 430 (2018) 2278–2287.
- [36] M. Fuxreiter, Fold or not to fold upon binding—does it really matter? *Curr. Opin. Struct. Biol.* 54 (2018) 19–25.
- [37] J. Garnier, J.-F. Gibrat, B. Robson, GOR secondary structure prediction method version IV, *Methods Enzymol* (1996) 540–553.
- [38] J. Dogan, S. Gianni, P. Jemth, The binding mechanisms of intrinsically disordered proteins, *Phys. Chem. Chem. Phys.* 16 (2014) 6323–6331.
- [39] S. Gianni, J. Dogan, P. Jemth, Coupled binding and folding of intrinsically disordered proteins: what can we learn from kinetics? *Curr. Opin. Struct. Biol.* 36 (2016) 18–24.
- [40] R.B. Berlow, H.J. Dyson, P.E. Wright, Hypersensitive termination of the hypoxic response by a disordered protein switch, *Nature* 543 (2017) 447–451.
- [41] M. Miskei, C. Antal, M. Fuxreiter, FuzDB: database of fuzzy complexes, a tool to develop stochastic structure–function relationships for protein complexes and higher-order assemblies, *Nucleic Acids Res.* 45 (2017) D228–D235.

- [42] S.L. Shammass, M.D. Crabtree, L. Dahal, B.I. Wicky, J. Clarke, Insights into coupled folding and binding mechanisms from kinetic studies, *J. Biol. Chem.* 291 (2016) 6689–6695.
- [43] J.J. Kohler, A. Schepartz, Kinetic studies of Fos:Jun:DNA complex formation: DNA binding prior to dimerization, *Biochemistry* 40 (2001) 130–142.
- [44] S.E. Pursglove, M. Fladvad, M. Bellanda, A. Moshref, M. Henriksson, J. Carey, et al., Biophysical properties of regions flanking the bHLH-Zip motif in the p22 Max protein, *Biochem. Biophys. Res. Commun.* 323 (2004) 750–759.
- [45] J.F. Naud, F.O. McDuff, S. Sauve, M. Montagne, B.A. Webb, S.P. Smith, et al., Structural and thermodynamical characterization of the complete p21 gene product of Max, *Biochemistry* 44 (2005) 12746–12758.
- [46] B.A. Shoemaker, J.J. Portman, P.G. Wolynes, Speeding molecular recognition by using the folding funnel: the fly-casting mechanism, *Proc. Natl. Acad. Sci. U. S. A.* 97 (2000) 8868–8873.
- [47] Y. Huang, Z. Liu, Kinetic advantage of intrinsically disordered proteins in coupled folding-binding process: a critical assessment of the “fly-casting” mechanism, *J. Mol. Biol.* 393 (2009) 1143–1159.
- [48] J. Schymkowitz, J. Borg, F. Stricher, R. Nys, F. Rousseau, L. Serrano, The FoldX web server: an online force field, *Nucleic Acids Res.* 33 (2005) W382–W388.
- [49] M. Guharoy, P. Bhowmick, M. Sallam, P. Tompa, Tripartite degrons confer diversity and specificity on regulated protein degradation in the ubiquitin–proteasome system, *Nat. Commun.* 7 (2016) 10239.
- [50] K. Tar, T. Dange, C. Yang, Y. Yao, A.L. Bulteau, E.F. Salcedo, et al., Proteasomes associated with the Blm10 activator protein antagonize mitochondrial fission through degradation of the fission protein Dnm1, *J. Biol. Chem.* 289 (2014) 12145–12156.
- [51] S. Bhattacharyya, J.P. Renn, H. Yu, J.F. Marko, A. Matouschek, An assay for 26S proteasome activity based on fluorescence anisotropy measurements of dye-labeled protein substrates, *Anal. Biochem.* 509 (2016) 50–59.
- [52] H.J. Dyson, P.E. Wright, Intrinsically unstructured proteins and their functions, *Nat. Rev. Mol. Cell Biol.* 6 (2005) 197–208.
- [53] J.J. Ward, J.S. Sodhi, L.J. McGuffin, B.F. Buxton, D.T. Jones, Prediction and functional analysis of native disorder in proteins from the three kingdoms of life, *J. Mol. Biol.* 337 (2004) 635–645.
- [54] F.X. Theillet, A. Binolfi, B. Bekei, A. Martorana, H.M. Rose, M. Stuiver, et al., Structural disorder of monomeric alpha-synuclein persists in mammalian cells, *Nature* 530 (2016) 45–50.
- [55] F.U. Hartl, Unfolding the chaperone story, *Mol. Biol. Cell* 28 (2017) 2919–2923.
- [56] C. Andresen, S. Helander, A. Lemak, C. Fares, V. Csizmok, J. Carlsson, et al., Transient structure and dynamics in the disordered c-Myc transactivation domain affect Bin1 binding, *Nucleic Acids Res.* 40 (2012) 6353–6366.
- [57] S. Helander, M. Montecchio, R. Pilstal, Y. Su, J. Kuruvilla, M. Elven, et al., Pre-anchoring of Pin1 to unphosphorylated c-Myc in a fuzzy complex regulates c-Myc activity, *Structure* 23 (2015) 2267–2279.
- [58] S. Boeynaems, S. Alberti, N.L. Fawzi, T. Mittag, M. Polymenidou, F. Rousseau, et al., Protein phase separation: a new phase in cell biology, *Trends Cell Biol.* 28 (2018) 420–435.
- [59] P. Li, S. Banjade, H.C. Cheng, S. Kim, B. Chen, L. Guo, et al., Phase transitions in the assembly of multivalent signalling proteins, *Nature* 483 (2012) 336–340.
- [60] H. Wu, M. Fuxreiter, The structure and dynamics of higher-order assemblies: amyloids, signalosomes, and granules, *Cell* 165 (2016) 1055–1066.
- [61] K.A. Burke, A.M. Janke, C.L. Rhine, N.L. Fawzi, Residue-by-residue view of in vitro FUS granules that bind the C-terminal domain of RNA polymerase II, *Mol. Cell* 60 (2015) 231–241.
- [62] A. Sultana, J.E. Lee, Measuring protein–protein and protein–nucleic acid interactions by bilayer interferometry, *Curr Protoc Protein Sci* 79 (2015) 19 [25 1-6].
- [63] A. Micsonai, F. Wien, E. Bulyaki, J. Kun, E. Moussong, Y.H. Lee, et al., BeStSel: a web server for accurate protein secondary structure prediction and fold recognition from the circular dichroism spectra, *Nucleic Acids Res.* 46 (2018) W315–W322.
- [64] A. Micsonai, F. Wien, L. Kernya, Y.H. Lee, Y. Goto, M. Refregiers, et al., Accurate secondary structure prediction and fold recognition for circular dichroism spectroscopy, *Proc. Natl. Acad. Sci. U. S. A.* 112 (2015) E3095–E3103.